CHAPTER 3

INCOHERENT SCATTERING CROSS SECTION

3.1 Introduction

Cross section in industrial radiography is defined as the measure of probability that a collision will occur between a beam of radiation and a particular particle. The cross section is usually measured in barns. However, the cross section is related to the attenuation coefficient such as the mass attenuation coefficient.

The applications of X-ray cross section data are mostly used and appreciated in medical diagnosis and therapy [3]. In the medical field especially in cancer therapy [3], the cross section is used to predict the dose at a given location within the patient. An example is the determination of how much of the primary γ-ray beam will arrive at the desired coordinates inside the patient or how much energy or dose will be deposited at the tumour site.

Hubbell [3] has listed the industrial applications of NDT. In the industrial sector, the knowledge on the mass attenuation coefficient helps in the design and operation of radiometric gauges to control rollers. The knowledge on mass energy absorption coefficient is also important in the radiation sterilization of medical supplies and also in irradiation curing of polymer plastics.

The total cross section when γ-rays interact with material is the sum over contributions from the principal photon interactions with the absorber [26]. However, the energy of the incident gamma ray will determine which process will occur as shown by Table 2.3.

In this research, the focus is only on Compton scattering. In describing the incoherent scattering, the cross section must be calculated. To include the effect of the attenuation processes, the cross section is calculated when gamma ray with energy from 0.1 keV until 100 MeV interacts with iron ^{56}Fe.

There are several numerical methods that are used in calculating the cross section. Hubbell [23] employed the Simpson rule to perform the integration. With this procedure, 1000 points were used in the integration and results were tabulated that are accurate to four decimal places. Another method is by using the trapezoidal method. The trapezoid method is possible since the equation is reasonably well behaved in the region $(0-\pi)$. Monte Carlo (MC) method is also used to evaluate the integral.

3.2 Incoherent Scattering Cross Section

In this research, we employ the Klein-Nishina formula for free electron Compton scattering [23] in which the Compton scattering cross section σ_c for a certain material is a function of both the energy of the incident photon and the scattering angle. The Klein-Nishina formula is a differential cross section of photons scattered from an unbound electron in lowest order of quantum electrodynamics. It is based on the Dirac electron theory without radiative correction. This formula was derived by Oscar Klein and Yoshio Nishina in 1928 based on the consideration of relativistic and quantum mechanical effects for the scattering radiation. At low frequency, the differential cross section reduces to the Thomson scattering but the differential cross section is normally applied to higher frequency sources such as X-ray and gamma radiation. Equation (3.1) is the bare Klein-Nishina formula which describes the differential cross section per unit solid angle per atom for the incoherent scattered photons,

$$\left(\frac{d\sigma_c}{d\Omega}\right)_{KN} = \frac{r_0}{2}\left\{\frac{1}{[1+\varepsilon(1-\cos\theta)]^2}\,[\,1+\cos^2\theta+\frac{\varepsilon^2(1-\cos\theta)^2}{1+\varepsilon(1-\cos\theta)}\,]\right\} \tag{3.1}$$

where r_0 is the classical electron radius, ε the gamma energy in MeV divided by 0.511 MeV, θ the scattering angle and $d\Omega$ the differential solid angle Ω in steradians which is $2\pi \sin\theta d\theta$. The expression (3.1) is only applicable for Compton scattering with free electrons. The cross section could be obtained analytically by integrating Equation (3.1) over all angles [17]. At $\varepsilon = 0$, the Klein-Nishina cross section σ_c will reduce to the classical Thomson scattering. The probability of the incoherent scattering event into a solid angle at the scattering angle θ is,

$$x = -\sin\left(\frac{\theta}{2}\right)\Big/\lambda \tag{3.2}$$

where (λ) Å is the photon wavelength that is $12398.52/\varepsilon(\text{eV})$ [3].

When gamma radiation interacts with a material, the electrons in the material are no longer considered as free electrons. They are bound electrons and the interaction is usually called as incoherent scattering. Hubbell [23] calculated the total incoherent scattering cross section for atoms ranging from *Z*=1 to 100 by multiplying the Klein-Nishina expression with tabulated values of the scattering functions, S. The scattering function is introduced as a correction to the free electron cross section in which it takes into consideration the effects of the bound electrons on the cross section. It is the probability that the atomic K-shell electrons receive momentum from the incident photons [27]. Thus, the total incoherent scattering cross section for bound-electron Compton scattering per atom is given as

$$\sigma_{incoh} = \int_{\theta=0}^{\theta=\pi} d\sigma_c(\theta) S(x,Z) \tag{3.3}$$

where the scattering functions $S(x,Z)$ is a function of x and the atomic number Z for the absorbing material.

There are different theoretical schemes available to calculate the incoherent scattering cross sections, such as incoherent scattering factor approximation, impulse approximation and S-matrix formalism [28]. Bergstrom [29] gave an overview of the theories used in Compton scattering calculations which describes how scattering deviates from scattering from free electrons, that is using solely Klein-Nishina expression to the effects of binding on Compton scattering. According to Bergstrom, Compton scattering from bound atomic electrons is also an elastic process which involve some changes in the energy of the internal state of the scatterer. The change of energy maybe due to the transitions process in atoms that occur either from one bound configuration to another i.e. an excitation or to a configuration where the atomic electrons have been promoted to the continuum when the atom experiencing ionisation process.

Roy et al. [28] used 'best' predicted cross sections for both elastic and inelastic scatterings. Their method estimated the magnitude of the various corrections such as dynamics effects, non-local exchange, electron correlation and relativistic effects. The incoherent scattering factor is determined by using the relationship, $F_{eff} + S$ where F_{eff} is known as the effective form factor calculated from the 'best' predicted cross sections for Rayleigh scattering. They have calculated the incoherent scattering cross sections for neon in the range 5-59 keV, carbon, aluminium, iron and copper in the energy range of 20-40 keV and momentum transfer range of 0.1 to about 5 $Å^{-1}$, by multiplying the Klein-Nishina cross section with the S values determined from the relationship. Their

results were found to agree well with the synchrotron experiments except for carbon where their estimations of correlation effects may be insufficient.

Verma et al. [6] measured the integral Compton scattering cross section at 279 keV for elements $26 \le Z \le 35$. Their results were found to agree quite well with the theoretical values which indicate that the K-shell electrons in the elements behave as free electrons and the integral incoherent scattering function becomes unity. However, they also mentioned that the results suffer from the contradictions from the relativistic calculations for incoherent scattering of photons by K-shell electrons which predicts non zero value of cross section at zero scattering angle. Using the same energy, Murty et al. [27] also measured the incoherently scattered photons by K-shell electrons in tungsten and erbium. They found that the differential cross section ratio for angles of 30^0 and 125^0 does not reach unity. However, there exists disagreement between theoretical and experimental results because the non-relativistic approximation was employed in the calculation and for that reason there is a need for a rigorous theory which is applicable to all scattering angles.

Kurucu [30] has made measurements for incoherent scattering cross section for 59.5 keV photon energy for elements $23 \le Z \le 51$. In this study, the scattering angles ranged from 30^0 to 140^0 with the detection using Ge(Li) detector. Investigation of electron binding effect to the incoherent scattering is essential since the influence of the electron binding effect is expected to be more significant in the lower range of energy. In his work, there is an agreement between the experimental results and theoretical values compiled by Hubbell [23] within the estimates of the experimental errors. Kurucu's results confirm that at low momentum transfer the binding effects are predominant. Another experiment was conducted using energy of 59.5 keV [31]. The

scatterers were iron, zinc and niobium. From the experiments they found out that there was a qualitative agreement between the experimental results and the theoretical values within the experimental errors. However, there was an increase in the deviation for heavy elements which demonstrates the electron binding effects. Simsek et al. [32] has also measured the inelastic scattering of 59.5 keV photons for elements titanium, iron and nickel. It was found out that the experimentally measured cross sections and the theoretical values disagree when the scattering angle decreases.

Umesh et al. [33] has measured the incoherent scattering cross section of various compounds that takes into consideration the attenuation cross section of its various atomic constituents and number of atoms of the element present as indicated by the chemical formula of the compound. The models used to calculate the incoherent scattering functions were Thomas-Fermi and Hartree-Fock. It was shown that the deviations between the bound electron cross sections and the free electron cross sections increase as Z increases at energy 279.2 and 514 keV. This shows that the electron binding effects increase when Z increases for a given energy. They also reported that at higher energies, binding effects show up only above $Z = 40$.

The Compton scattering at 662 keV, which is from Cs-127 source was also investigated for various elements specifically copper, zinc, cadmium, tin, tungsten, platinum, lead and uranium [34] where there were deviations from the free electron behaviour for heavy elements and at scattering angles smaller than 15^0.

When we calculate the cross section for iron material, the scattering functions are included due to bound electrons in the element of ${}^{56}F$. The values of the scattering function for pure iron are adopted from Hubbell [23]. Hubbell calculated the scattering functions using theoretical models and approximations for instance, using Pauling and

Sherman method, Thomas-Fermi Statistical method and Hartree-Fock Model [23]. The integration is done from 0 to π. Hence, the differential incoherent scattering cross section per atom for bound electrons is given as,

$$\frac{d\sigma_{incoh}}{d\Omega} = \left(\frac{d\sigma_c}{d\Omega}\right)_{KN} S(x,Z) \tag{3.4}$$

where *Z* is the atomic number for the absorbing material.

3.3 Incoherent Scattering Cross Section for Iron and Carbon Steel

Our numerical method is different from the previous calculation by Hubbell [23] whereby we have used the Gauss-Legendre method in the integration. The integration is done with 10 000 points by using Equation (3.4). Scattering function is interpolated from tables in Hubbell [23]. Weighting factor is also taken into consideration in this method. Mork [23] has combined the radiative and double-Compton correction to give meaningful corrections to the Klein-Nishina Compton scattering cross section. These corrections are applied in our calculations. Hence, the cross section with the correction is given as

$$\sigma_{incoh}(corr) = \sigma_{incoh}\left(1+\Delta\sigma_{KN}^{M}\right) \tag{3.5}$$

where $\Delta\sigma_{KN}^{M}$ is the Mork correction factor.

In this work, three sets of calculations are illustrated. The calculations involve 1) the interaction of γ radiation with free electrons i.e. the incoherent Compton scattering, 2) the interaction of γ radiation with the valence electrons and 3) the interaction of γ radiation with bound electrons. The photoelectric absorption cross section for steel can be obtained from the XCOM online code [14]. Using this code, the cross sections for

photoelectric effect in the energy spectrum of Iridium-192 are obtained from the XCOM.

Figure 3.1 shows the incoherent scattering cross section that we obtain from the calculations for ^{56}Fe. It has a Gauss-type distribution graph. The cross section is expressed in terms of barns/atom. The interaction starts to increase at energy 1.5 keV and reach its maximum cross section at 50 keV which is 12.63 barns. The difference between Hubbell [23] and the calculated cross sections at this particular energy is about 0.5%. From the graph, the cross section starts to decrease at energy 60 keV.

Figure 3.2 shows the difference between Hubbell and the calculated cross section shown in Figure 3.1 in the form of percentage (%). The range of difference is from 0% which is at energy 400 keV to 1.0% at energy 20 keV. The error starts increasing at energy 0.6 keV with percentage error 0.2%. The error keeps on increasing until it reached the energy 20 keV with percentage error 1%. At energy 300 keV, the error starts to drop until it reaches zero at energy 400 keV. The error starts to rise again at energy 500 keV. At energy 1.0×10^5 keV, the percentage error is 0.9%. The numerical errors originate from two sources; the integration and the interpolation routines. From the results, the differences between Hubbell and calculated cross section are not significant. This implies that the calculated values are in good agreement with the published results.

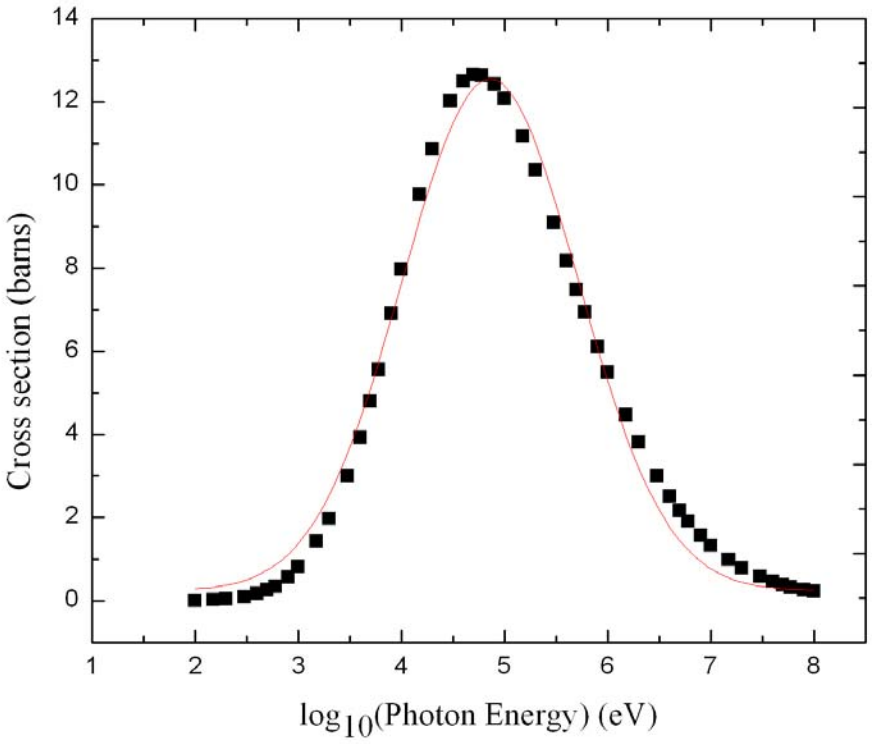

Figure 3.1 Incoherent scattering cross section as a function of photon energy for iron. The Gaussian fit is determined as $\sigma_{incoh} = 0.98829 + \left(26.288/\left(1.70511\sqrt{\pi/2}\right)\right)exp\left(-2\left(\left(x-4.86019\right)/1.70511\right)^2\right)$.

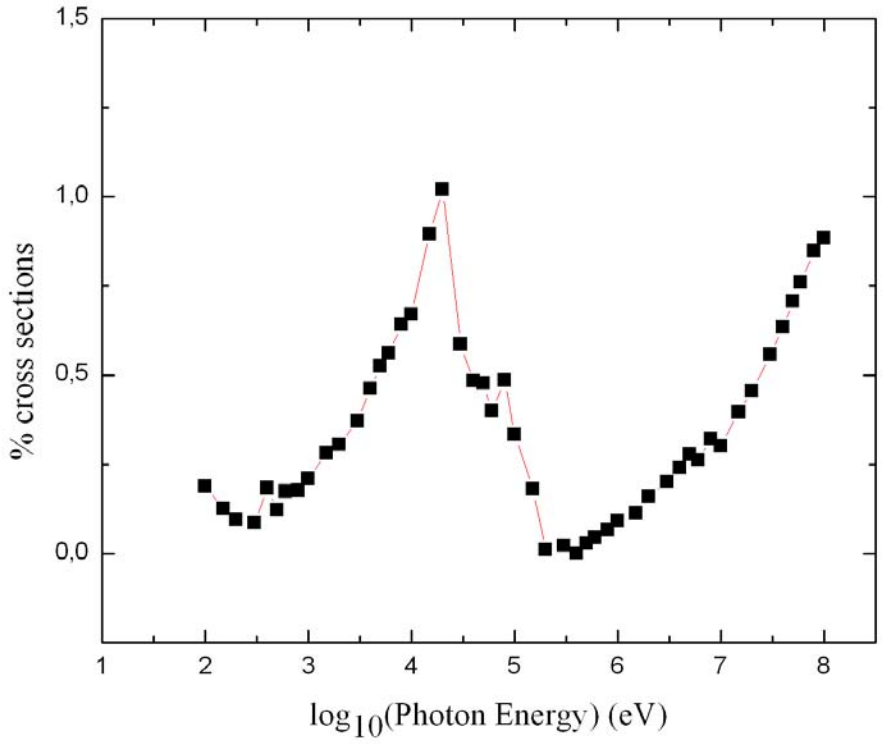

Figure 3.2 Error (%) of cross section for iron between Hubbell [23] and Figure 3.1.

Figure 3.3 shows the cross section of every element in the carbon steel sample (see Chapter 4) that we used in our experiments. The elements namely iron, carbon, chromium, copper, manganese, molybdenum, nickel, phosphorus, sulphur, silicon, aluminium, calcium, tin and nitrogen. Tin shows the largest cross section while carbon has the smallest cross section compare to other elements in the material.

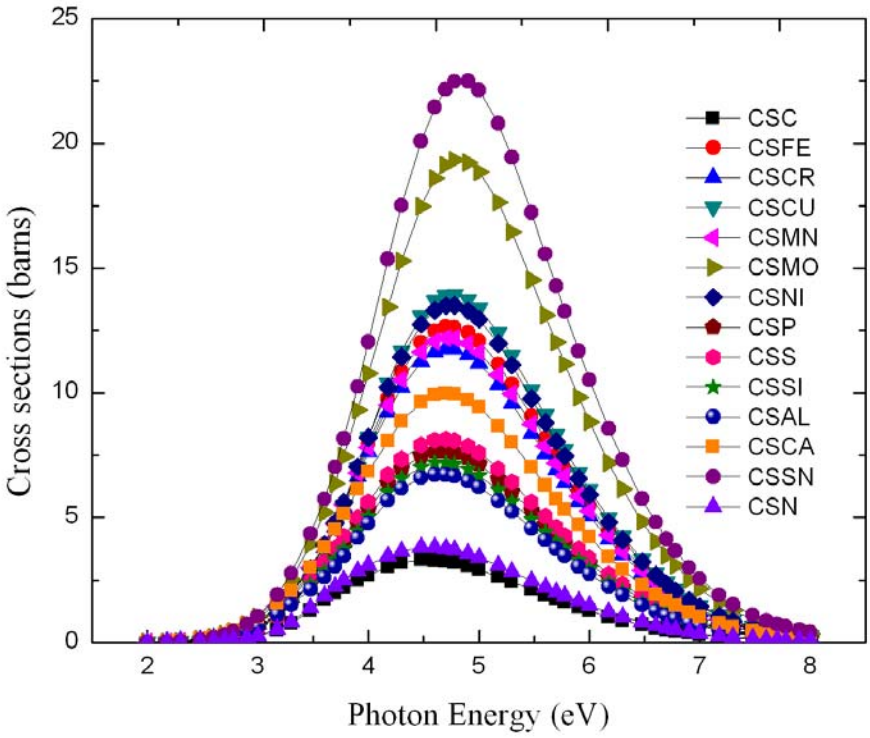

Figure 3.3 Cross section of all elements in the carbon steel sample (see Chapter 4).

Tin has the mass number 119 and the atomic number is 50 while carbon has mass number 12 and the atomic number is 6. Since the size of tin (atomic radius is 140 pm) is larger than the size of carbon (atomic radius is 70 pm) [17], the probability of the γ-tin interaction is high. Also, the number of electrons which acts as the scattering centres is higher in tin than in carbon.

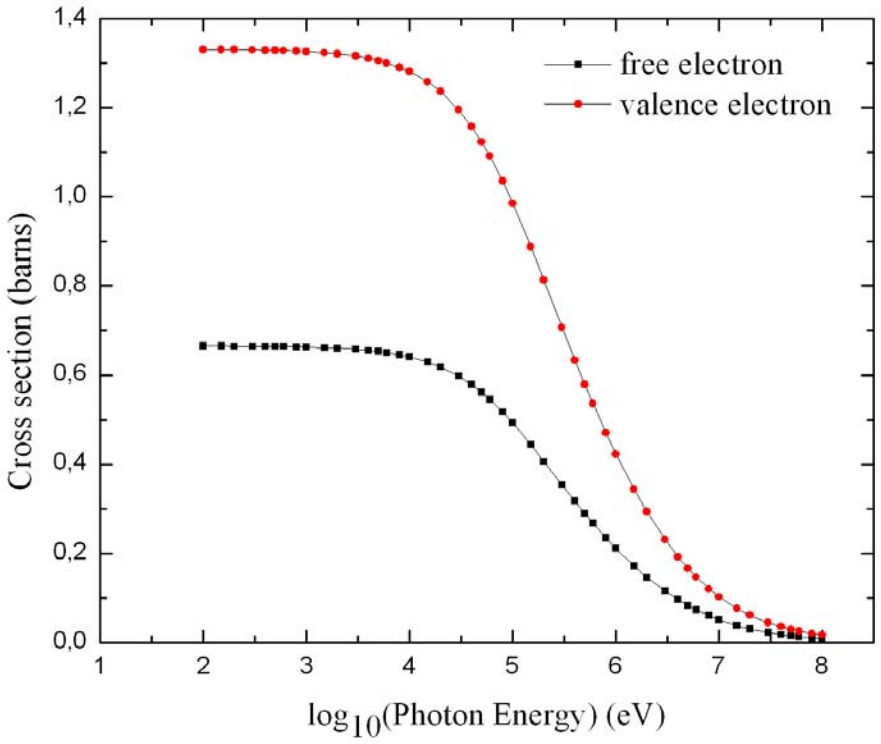

Figure 3.4 Cross section for ^{56}Fe with free and valence electrons.

Figure 3.4 shows the cross section for ^{56}Fe for the interaction of photons with free electrons and valence electrons. The value of the cross section for free electrons at energy 100 eV is 0.66 barns. However, at the same energy, cross section for the valence electrons increases to twice the value of cross section of free electrons which is 1.33 barns. There are total of 26 electrons in the atom of ^{56}Fe and of these, two are the valence electrons on the outer shell. The remaining 24 electrons are tightly bound in the inner shells. When the material is irradiated with γ radiation, the photons will interact with the valence electrons. Hence, for this case, the bare Klein-Nishina formula must be counted twice due to the valence electrons in the iron. The cross section for free

electrons and valence electrons remains constant at 0.66 barns and 1.32 barns respectively in the energy range 100 eV until 2 keV.

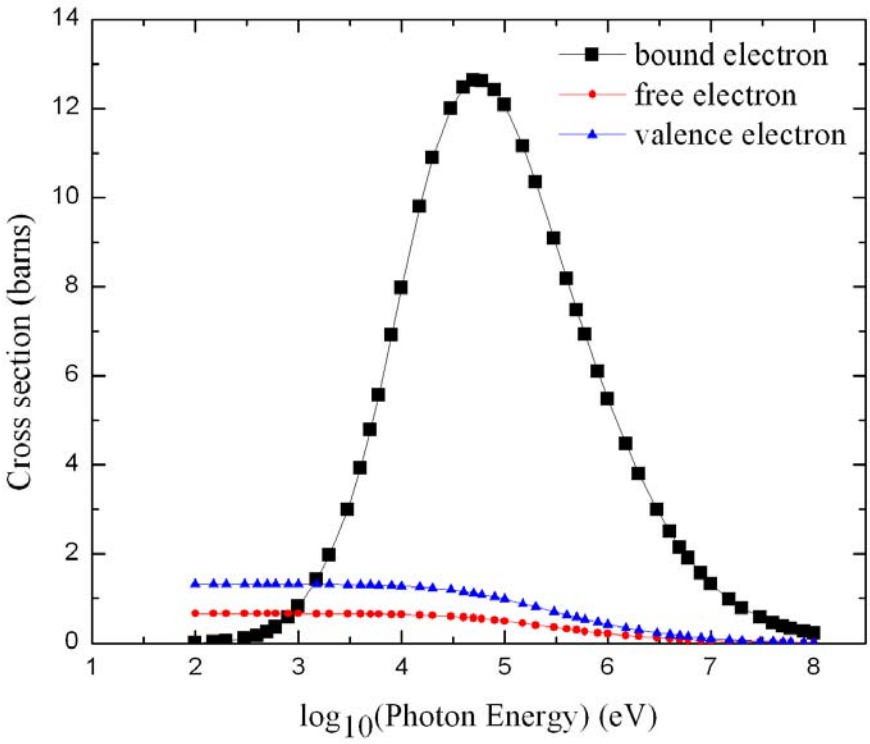

Figure 3.5 Cross section for ^{56}Fe with three different conditions; 1) free electrons, 2) two (2) valence electrons and 3) bound electrons.

Figure 3.5 shows the comparison of the cross section of ^{56}Fe from three different conditions; photons interacting with free electrons, interaction with only two valence electrons and bound electrons. It shows that the cross section of the photons interacting with free electrons using the bare Klein-Nishina formulation does not exhibit the behaviour of the total cross section as shown in Figure 3.1 especially at lower energies. Below 5 keV, the cross section of the γ-free electrons and γ-valence electrons gradually become constant. At 2 keV both cross sections for free electrons and

valence electrons interactions become constant which are 0.66 barns and 1.32 barns respectively. However when considering the bound electron effects, the cross section of the γ-bound electrons increases by one order of magnitude with respect to the bare Klein-Nishina case. It has a similar Gauss-type profile as in Figure 3.1. We can easily observe that the cross section is heavily underestimated for the γ-free electrons and γ-valence electrons interactions.

We have clearly show that the use of the bare Klein-Nishina formula is not accurate enough for calculating Compton scattering in complex structures. The scattering function must be integrated in the bare Klein-Nishina formula to include the influence of bound electrons.

3.4 Theoretical Attenuation Coefficient of Carbon Steel

In obtaining the total linear attenuation coefficient, Equation (3.6) below is used,

$$\mu_{linear}^{i}(E) = \sigma_i(E_j)N_i \ \text{cm}^{-1} \tag{3.6}$$

where the total cross section, σ_i is in barns and the number density of the scattering centre N_i in cm^{-3} at a particular photon energy E_j. The total cross section consists of the contributions from photoelectric absorption and incoherent scattering processes. The coherent scattering process is not taken into consideration because the process does not involve any changes in the energy of the photon. The number density of any element in a sample is calculated using the following equation:

$$N_i = \frac{\text{Avogadro number}}{\text{atomic mass}} \times \text{density} \quad \text{atoms/cm}^3. \tag{3.7}$$

The mass attenuation coefficient can be calculated using the following formula:

$$\mu_{mass}(E) = \frac{\mu_{linear}(E)}{\rho}. \tag{3.8}$$

The density of each element in the carbon steel sample is taken from reference [11]. According to [13], there are eight main energies in the decay spectrum of Iridium-192. We adopt seven most prominent decay lines from Table 2.2 as listed in Table 3.1 below. The mass attenuation coefficients are taken from XCOM but the linear attenuation coefficients are calculated using Equation (3.8). The linear attenuation coefficient is the product of mass attenuation coefficient and the (bulk) density of the sample. In this calculation we estimate the density of carbon steel sample as $8.08156\ \mathrm{g/cm^3}$ where the weight of the sample is $776.8\,g$ and the volume $96.12\,\mathrm{cm^3}$. The theoretical linear attenuation coefficient of our carbon steel sample can be estimated by a weighted average of the attenuation coefficients in Table 3.1 over the Iridium-192 spectrum. Thus, the effective linear attenuation coefficient of the carbon steel sample is

$$\mu_{linear} = 0.231\ \mathrm{cm^{-1}}. \tag{3.9}$$

Table 3.1 Mass attenuation coefficient for the prominent energies in Iridium-192 spectrum adopted from Table 2.2.

Energy, E (keV)	I_g (%)	$\mu_{mass}(E)\ (\mathrm{cm^2/g})$	$\mu_{linear}(E)\ (\mathrm{cm^{-1}})$
295.96	0.287	0.10590	0.85583720
308.46	0.300	0.10360	0.83724962
316.51	0.828	0.10230	0.82674359
468.07	0.478	0.08494	0.68644771
588.58	0.045	0.07651	0.61832016
604.41	0.082	0.07558	0.60708679
612.47	0.053	0.07512	0.56918427